processes

MDPI

Article

Enhancing the Efficiency of Fluidized Bed Reactors for Biomass Torrefaction

Fouzi Tabet [1], Oleg Milovanov [2], Dmitry Klimov [2], Artem Ryzhenkov [2], Sergey Grigoriev [2], Rafail Isemin [3,*], Alexander Mikhalev [3], Evgeny Pitsukha [4] and Yury Teplitskii [4]

[1] Opti'Tech, Schletterstrasse 12, 04107 Leipzig, Germany
[2] Wear Resistance Center, National Research University "Moscow Power Engineering Institute", 111250 Moscow, Russia
[3] Clean Energy LLC, 392032 Tambov, Russia
[4] A.V. Luikov Heat and Mass Transfer Institute, National Academy of Sciences of Belarus, 220072 Minsk, Belarus
* Correspondence: risemin@gmail.com

Abstract

This paper examines the study of an advanced design for a continuously operating fluidized bed reactor applied to sunflower husk torrefaction in a superheated steam environment, which is simulated in a cold model of the reactor. The simulated reactor has a diameter of 0.3 m and contains six vertical baffles installed along the reactor walls, providing loop-like movement of crushed husk particles from the reactor loading point to the reactor biomass unloading point. The residence time of crushed sunflower husk biomass particles in the reactor was studied by introducing colored biomass particles into the bed; these particles had the same mass and size as the undyed material. According to modeling results, replacing superheated steam with room-temperature air in the "cold" model may not lead to significant changes in the hydrodynamics of the fluidized bed or their effect on particle mixing. Experiments were conducted at an air velocity of 0.6 m/s relative to the cross-section of the empty apparatus, which is 3.5-fold greater than the minimum fluidization velocity. Samples were collected at the reactor outlet and dissolved in distilled water. The transparency of the resulting solution was measured using a KFK-3 photometer, and the amount of colored substance in each sample was determined accordingly. The most probable average residence time of biomass particles in the cold model amounted to 6–8 min at a Peclet number of 47. To ensure full operation of the torrefaction reactor under ideal plug-flow conditions, the reactor must be equipped with 24 baffles. The residence time of biomass particles required for optimal operation of the reactor was estimated to 24–32 min, which may be sufficient to produce biochar with a high calorific value, suitable for co-firing with coal.

Keywords: sunflower husks; torrefaction; fluidized bed; "cold" model

Check for updates

Academic Editor: Juan Francisco García Martín

Received: 25 November 2025
Revised: 11 February 2026
Accepted: 13 February 2026
Published: 17 February 2026

Copyright: © 2026 by the authors. Licensee MDPI, Basel, Switzerland. This article is an open access article distributed under the terms and conditions of the Creative Commons Attribution (CC BY) license.

1. Introduction

Agricultural productions generate a significant number of secondary products and waste, which are currently used as fuel for the production of thermal and electrical energy [1].

Sunflower (*Helianthus annuus*) is a herbaceous plant of the Asteraceae family, widely cultivated worldwide due to its relatively short growth cycle, high drought resistance, and adaptability to diverse soil conditions. The leading sunflower-producing countries, as well

as producers of sunflower-derived products, are the Russian Federation, Ukraine, and Argentina, which together account for approximately half of the global sunflower yield [2].

Sunflower husk (SFH) accounts for 45–60% of the seed mass, depending on sunflower variety [2]. SFH is separated from the kernel to improve seed pressing efficiency and increase the yields of sunflower oil. As a by-product of sunflower oil production, SFH is widely used in animal feed production; however, its application for energy generation remains limited [3], despite its relatively high calorific value.

The processing of agricultural waste into biofuels and/or bioenergy may represent an attractive alternative for more sustainable waste utilization, reducing environmental impacts while also generating economic and social benefits. For example, studies of physical and chemical properties of tomato processing waste [4] have demonstrated its suitability for use as solid biofuel, particularly in the energy sector of large power plants.

The concept of utilizing agro-industrial waste for energy production through thermochemical processes is not new. However, since such feedstocks are typically characterized by low calorific value, high moisture content, hygroscopicity, and susceptibility to decay, high costs associated with handling, storage, and processing have thus far constrained progress in this sector [5].

Over the past decade, new findings suggest that torrefaction technology may provide a viable pretreatment option to overcome the aforementioned barriers and convert low-value biomass feedstock into material suitable for energy applications, such as combustion and gasification [6]. Specifically, torrefaction yields a hydrophobic product that: (1) can be stored outdoors; (2) reduces biological degradation; (3) allows fuel standardization by producing non-fossil solid fuel with predetermined physical and chemical properties regardless of initial biomass composition; (4) increases calorific value compared with raw biomass; and (5) decreases the grinding cost of torrefied biomass, with is more fragile than the original biomass. These advantages significantly facilitate the process of co-firing of torrefied biomass in coal-fired power plants.

Furthermore, since agro-industrial wastes such as SFH are generated in large quantities at their processing plants, torrefaction of these by-products can be carried out on-site, reducing transportation costs and improving economic feasibility of thermal treatment.

The torrefaction of agricultural waste (tomato peels) in a reactor with a fluidized bed of inert material (quartz sand) was already investigated by other authors [4,5], demonstrating that fluidized bed technology may be more suitable than fixed bed technology for overcoming adverse exothermic effects associated with thermal degradation of non-woody biomass, which tends to ignite or char easily during torrefaction.

The carrier gas bringing the bed particles into a fluidized state can be composed of nitrogen, air [6], or a mixture of nitrogen and air [7]. Alternatively, torrefaction can be carried out in a steam environment. Biochar produced by steam torrefaction may contain less carbon than biochar obtained through hydrothermal carbonization, while its properties may be similar to semicoke produced by dry carbonization in a closed reactor. However, carbon losses occurring with the process liquid may be lower during steam carbonization than during carbonization in water, and energy efficiency of steam torrefaction may be higher than hydrothermal carbonization [8]. The use of superheated steam as a torrefaction agent holds significant interest, enabling fast and uniform process and allowing easy removal of volatile compounds [9,10]. Steam torrefaction follows an initial stage of biomass drying with superheated steam at atmospheric pressure. After drying, the biomass heating subsequently takes place at 220–250 °C in an oxygen-free steam environment. Superheated steam torrefaction may offer several advantages over conventional torrefaction, since superheated steam provides superior heat-transfer properties, its heat capacity is twice as high as that of nitrogen, and its kinematic viscosity is twice as low at the same temperature.

In previous studies, the authors demonstrated the feasibility of using superheated steam for torrefaction in a fluidized bed reactor for potato skin [11], olive leaves, and olive pomace [12]. The application of inert material, such as quartz sand, as fluidizing medium for torrefaction in a fluidized bed may require additional processing stages for subsequent separation of torrefied biomass (biochar) from the inert material. Clearly, recycling biochar particles obtained from the same material being torrefied for their use as fluidizing medium may constitute a preferable option [7,13].

Additionally, a limiting factor to the commercial use of torrefaction technology is the high cost of the process. According to estimates [14], the costs of biomass torrefaction per unit of torrefied biomass may be shared as follows: raw material 45%, personnel costs 3–13%, energy costs 3–10%, depreciation costs 12–17%, other 22–40%. The high share of raw material costs is associated with the requirement for drying the initial biomass. These costs can be significantly reduced, either by using dry biomass, or by applying spent superheated water steam used in the torrefaction process for the pretreatment stage of biomass drying.

Furthermore, the application of fluidized bed technology for biomass torrefaction faces certain limitations: since fluidized bed reactors may operate optimally under conditions of ideal mixing, uniform biomass treatment cannot be achieved during continuous feeding and discharge [10]. Accordingly, in order to reduce the degree of non-uniformity in biomass treatment within the fluidized bed, the reactor must operate in batch mode [4,5], which decreases the overall throughput of the torrefaction system.

In order to overcome these limitations, researchers and developers of fluidized bed reactors have proposed various methods to improve the efficiency and performance of this equipment. One such method is the addition of partitions within the reactor, which is frequently mentioned in the literature and widely applied in the industry. These partitions are mainly used in dense fluidized beds operating at low velocities. Based on their shape and arrangement, the partitions described in the literature can be divided into three main groups: horizontal partitions, vertical partitions, and fixed inserts. Among these three categories of partitions, horizontal partitions have been the most extensively studied, both experimentally and through computational fluid dynamics [15]. Partitions can reduce the bypassing of solid particles in circulating fluidized beds, limit back-mixing of gases, enhance particle mixing in a specific direction according to the partition's design, and limit the back-mixing of particles within the fluidized bed [16]. In particular, horizontal partitions, tubes, or inserts can be added in order to reduce the size and rate of formation of bubbles in fluidized bed reactors. In particular, large gas bubbles formed in fluidized bed reactors reduce the intensity of heat and mass transfer and decrease the contact time between solid particles and gases, lowering the overall efficiency of the fluidized-bed reactor [17]. In this regard, Phuakpunk et al. [18] researched the influence of bubble coalescence in fluidized-bed gasifiers along with the potential use of louvered partitions to mitigate this effect, demonstrating improved biomass distribution while maintaining the overall pressure drop and identifying optimal inlet gas velocity to achieve enhanced performance [19]. N. Liu et al. [20] studied the effect of louvered partitions on the hydrogenation of silicon tetrachloride in fluidized beds, obtaining improved uniformity in the movement of gas and solid particles, reducing gas back-mixing, and increasing the conversion rate of gaseous reactants. Horizontal fluidized-bed reactors are becoming increasingly popular [21,22]. However, in these reactors, biomass particles spend variable amounts of time in the system, which reduces the uniformity of their treatment. This issue results from the superposition of fluid movements of direct convective transport and dispersion in all directions. Nevertheless, in these studies, vertical partitions were placed within an elongated horizontal fluidized bed design, the construction of which may require a reactor of considerable dimensions.

In horizontal reactors equipped with vertical partitions, the processing of feedstock particles with a wide particle size distribution may lead to operational challenges. Increasing the height of the vertical partitions may be necessary to reduce particle transport velocity from the loading zone to the discharge zone; however, this design choice may increase the risk of accumulation of large particles in the lower regions adjacent to the partitions. Such a design, when applied to the torrefaction process, may result in particle mass and size change, along with melting and subsequent agglomeration of biomass particles, whereas these adverse effects may further increase the probability of accumulation of large particles and agglomerates near lower sections of vertical baffles, potentially resulting in disruption of reactor operation.

In view of these issues, we proposed placing vertical partitions along the walls of a cylindrical apparatus, following a specific design, where the material follows a looped path from the feed to the discharge point, which may allow for a significant reduction in the reactor size for torrefaction. The transfer of biomass particles from one reactor section to another may occur along the entire height of the baffle through the gap between the baffle and the reactor wall. Hence, the improved design may reduce the probability of particle agglomeration and accumulation in the lower part of the proposed reactor. Additionally, if the design is implemented in an industrial reactor, these partitions may be heated, enabling intensified biomass torrefaction. Furthermore, the cylindrical shape of the reactor may allow for more uniform gas distribution at the inlet of the fluidized bed, compared with a long horizontal reactor. In long horizontal reactors, ensuring uniform inlet distribution of fluidizing gases may require the gas distributor grid to be segmented along the reactor length, with independent control of gas supply to each section. In the absence of such a regulation system, achieving homogeneous fluidization over the entire reactor length may become extremely challenging. Non-uniform fluidization along the length of a horizontal reactor may lead to deterioration in the quality of the produced biochar, while also undermining the operational stability of the reactor due to the increased risk of biomass sintering.

The aim of the present study is to implement a cold model for the estimation of optimal process parameters applied for the torrefaction of sunflower husk (SFH), based on the estimated residence time of biomass particles in a cylindrical reactor with vertical baffles installed along the reactor walls.

2. Materials and Methods

SFH was obtained from JSC "Ecooil," Tambov, Russia. After milling, the husk had the following fractional composition: particles smaller than 1 mm 3.2%, particles sized 1–1.2 mm 55.0%, and particles larger than 1.2 mm 41.8%. The bulk density of SFH was 221 kg/m^3.

The analysis of SFH (as received) was performed using standard method ASTM E 870-82 [23], and elemental analysis was conducted with a TruSpec CHNS analyzer (LECO Corporation, St. Joseph, MI, USA). The carbon, hydrogen, nitrogen, and oxygen contents in SFH were 48.2%, 5.71%, 2.06%, and 35.07%, respectively. The feedstock parameters were as follows: moisture content 7.09%, volatile matter content 67.74%, fixed carbon content 22.09%, and ash content 3.08%. The higher heating value (HHV) of SFH on a dry, ash-free basis amounted to 19.51 MJ/kg (±0.1%). The calorific value of biomass was determined using an ABK-1V bomb calorimeter (Investment Scientific-Production Company "Russian Energy Technologies" LLC, Moscow, Russia).

Due to the difficulty of fluidizing SFH biomass in its original state, biomass grinding was required. During the fluidization of untreated sunflower husk, significant pressure-drop fluctuations occurred as the velocity of the fluidizing gas increased. These pressure-

drop surges were not reproducible in individual experiments, as unstable channels and voids formed along the bed height. On the other hand, ground SHF was easily fluidized, and particle entrainment was minimal.

Experimental setup

The study of the torrefaction process of SFH was carried out using an experimental setup presented in Figure 1, which has already been applied in previous research [11].

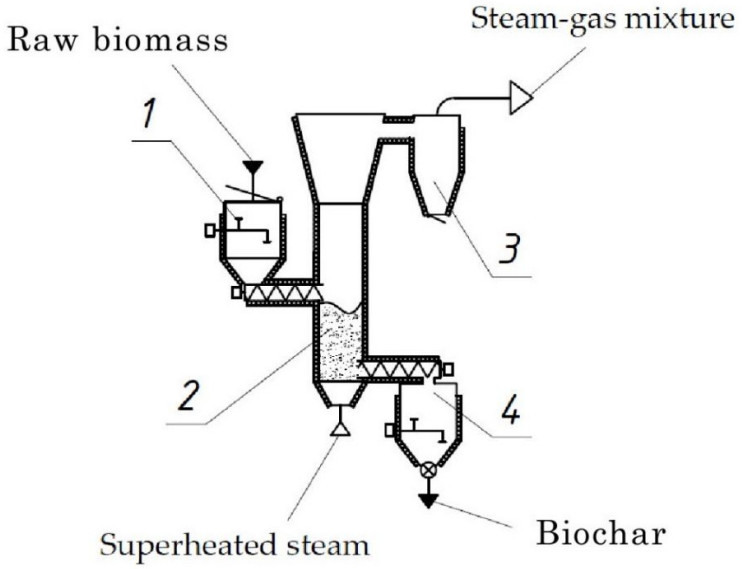

Figure 1. Diagram of the experimental setup of the superheated steam fluidized bed reactor [11].

The setup includes: inlet hopper for feedstock (1), batch reactor with a fluidized bed (2), cyclone for separating the mixture of spent steam and gaseous torrefaction products (3), and outlet hopper for torrefied biomass (4). The system is also equipped with a steam electric boiler, an electric superheater, and a water condenser for spent steam. The torrefaction process was carried out at temperatures of 200 °C, 250 °C, and 300 °C. Torrefaction temperature and duration were set at the same levels as previous studies performed on torrefaction of potato skins [11], as well as olive leaves and olive pomace [12].

The reactor (2), equipped with a transparent borosilicate glass insert, allowing visual monitoring of the biomass fluidization process, had a diameter of 80 mm, and was fitted with a bubbling-type gas distribution grid located at the bottom. The bed was fluidized by steam at a pressure not exceeding 0.2 MPa, supplied by an electric boiler. The steam temperature at the outlet of the electric boiler was 120 °C. The steam was heated further in the electric superheater, so that the steam temperature reached experimental targets of 200, 250, and 300 °C. The maximum steam flow rate was 20 kg/h, and the steam flow rate was regulated using a valve. The pressure drop across the fluidized bed was measured using a micromanometer (Testo 525, Testo SE & Co. KGaA, Titisee-Neustadt, Germany). At the onset of each experiment, 800 g of biomass sample were loaded into the reactor. Torrefied biomass (biochar) exiting the reactor was discharged into the outlet hopper (4). This device was sealed hermetically to prevent contact between air and hot torrefied biomass. Hot torrefied biomass was cooled with cold nitrogen to a temperature of 20 °C. The cooled biomass was subsequently unloaded from the outlet hopper (4) for further analysis. Each experiment, characterized with target temperature and treatment duration, was repeated five times, whereas experimental results deviated from the mean by no more than 5%.

Cold model of the advanced partitioned reactor design

The cold model was based on a simulated reactor design, with reactor diameter set to 0.3 m. In order to ensure sufficient residence time of biomass particles in the fluidized

bed reactor, it was proposed to install a set of vertical partitions inside the reactor. These partitions were positioned in such a way that a gap existed between the partitions and the reactor walls (Figure 2). This specific arrangement facilitated the loop-like movement of biomass particles from the inlet to the outlet of the reactor. Between any two partitions, the reactor operated under conditions of ideal mixing, which was monitored visually through the transparent walls of the reactor). Overall, however, the reactor design aimed at providing the necessary residence time for each biomass particle. Preliminary studies using this reactor had been conducted previously [24].

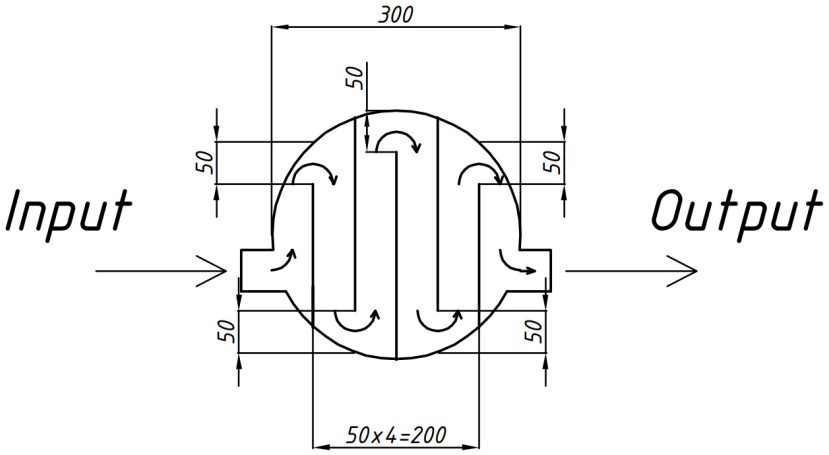

Figure 2. Schematic arrangement of the vertical partition set (top view) [24].

The distance between the vertical partitions was 50 mm, which is several times greater than the size of individual biomass particles, with more than 50% of the biomass particles having a size in the range of 1–1.2 mm. The reactor was incorporated into an apparatus for cold modeling of the motion of biomass particles, as represented in Figure 3.

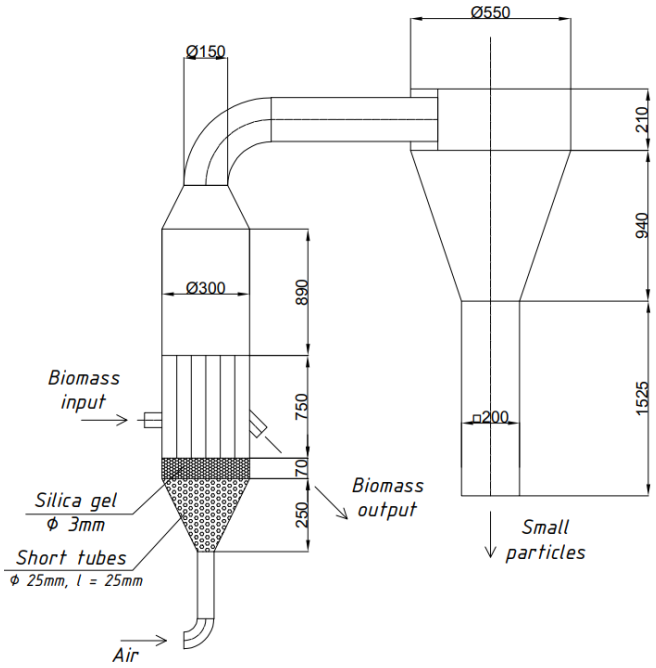

Figure 3. Diagram of the cold modeling apparatus (side view) [24].

The cold modeling apparatus comprised a cylindrical container with a diameter of 300 mm and height of 1640 mm. The container was set on an air distribution grid, composed of a layer of 3 mm silica gel particles sandwiched between two screens. The

cold modeling apparatus was also equipped with biomass loading and discharge units. A cyclone separator was installed downstream of the fluidized bed apparatus to separate biomass particles carried out of the bed by the air flow. Inside the fluidized bed container, a set of vertical partitions was placed, the schematic arrangement of which is shown in Figure 2.

In the cold modeling apparatus, air was used to fluidize SFH particles. In the cold model, superheated steam was substituted with air at 20 °C. The onset velocity of fluidization of cold SFH particles in air was calculated using the force balance between particle weight and drag, based on Ergun's equation [25]:

$$\rho_s g(1-\varepsilon) = 150\frac{(1-\varepsilon)^2}{\varepsilon^3}\frac{\mu_f u_{mf}}{d^2} + 1.75\frac{\rho_f u_{mf}^2(1-\varepsilon)}{\varepsilon^3 d} \quad (1)$$

The solution of Equation (1) with respect to u_{mf}, was as follows:

$$u_{mf} = \frac{\mu_f}{\rho_f d}\left(-42.8(1-\varepsilon) + \sqrt{1836(1-\varepsilon)^2 + 0.57\varepsilon^3 Ar}\right) \quad (2)$$

Interpolation of Equation (2) at $\varepsilon = 0.4$ provided the following formula:

$$u_{mf} = \frac{\nu_f}{d}\frac{Ar}{1400 + 5.22\sqrt{Ar}} \quad (3)$$

After grinding, the fractions of husk particles were distributed as follows: smaller than 1 mm $\varphi 1 = 3.2\%$, range 1–1.2 mm $\varphi 2 = 55.0\%$, and larger than 1.2 mm $\varphi 3 = 41.8\%$. The equivalent particle size was $d = \Sigma \varphi_i d_i = 1.08$ mm. For SFH particles fluidized with air at 20 °C, the following parameters were obtained: Archimedes number Ar = 29,080, Reynolds number Re = 12.69, and minimum fluidization velocity 0.177 m/s. Comparatively, for SFH particles fluidized with superheated steam at 200 °C: Ar = 57,770, Re = 21.76, and minimum fluidization velocity 0.172 m/s; for SFH particles fluidized with superheated steam at 250 °C: Ar = 40,300, Re = 16.46, minimum fluidization velocity 0.165 m/s; for SFH particles fluidized with superheated steam at 300 °C: Ar = 29,800, Re = 12.95, and minimum fluidization velocity 0.158 m/s. These calculations indicate that replacing superheated steam with room-temperature air in the cold model may not lead to significant changes in the hydrodynamics of the fluidized bed, or in the nature of particle mixing.

In order to study the residence time of SFH particles in the cold model apparatus, uncolored SFH particles were spiked with particles dyed by means of a water-soluble colorant, which, after drying, were identical in mass and size to undyed SFH particles.

Experiments were conducted at an air velocity of 0.6 m/s, referenced to the cross-section of the empty apparatus. A batch of dyed particles weighing 7.5 kg was continuously introduced into the bed over a period of 15 min. The height of the stationary layer of husk particles was 100 mm.

At the outlet of the apparatus, samples of husk particles with a volume of 50 mL were collected at time intervals of 30 s. From each sample, a 1 g sample was taken and dissolved in 40 mL of distilled water. The transparency of the obtained solution was then measured using a KFK-3 photometer (Zagorsk Optical and Mechanical Plant, JSC, Zagorsk, Russia), which was used to estimate the amount of dyed material in the sample.

The relationship between the ratio of colored and original SFH particles and the transparency of the solution was assessed in order to establish a calibration curve (Figure 4), correlating the transparency of the solution with the concentration of dyed material in the sample. For this purpose, samples were prepared at 10% intervals, weighing 1 g each, and containing approximately 13,000 particles of colored and original SFH particles in the range 0–100%, with 0% accounting for pure undyed SFH particles; and 100% accounting

for pure dyed SFH particles., which were then diluted with 40 mL of distilled water. The solution was left to stand for 30 min, filtered through a metal mesh, and allowed to settle for 24 h. The solution was subsequently placed in a KFK-3 photometer cuvette, and its transparency was determined according to the instrument's methodology, using a light source wavelength of 650.4 nm, corresponding to the red color of the solution.

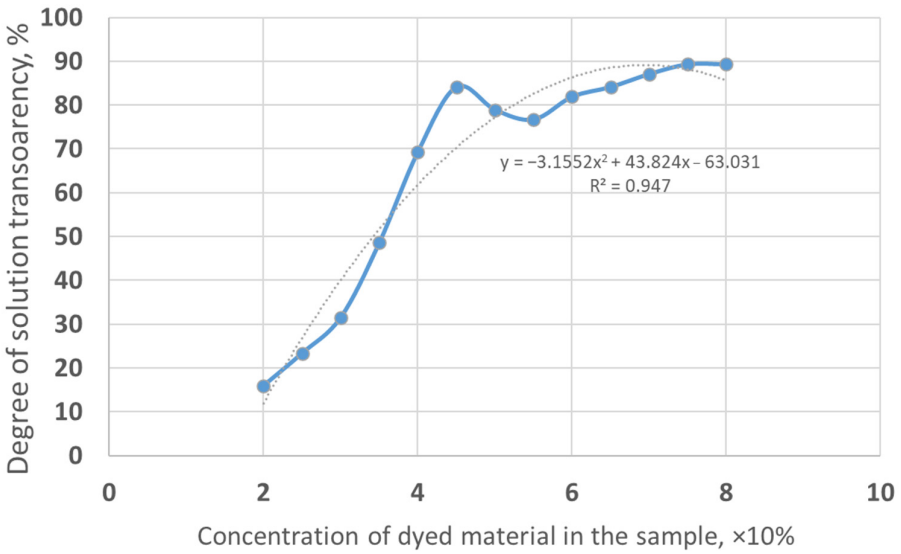

Figure 4. Calibration curve correlating transparency of the solution with the concentration of dyed SFH particles in the sample.

Calibration curves were also constructed for solutions with settling times of 60, 90, 120, 150, 180, and 210 min; analysis of the curves showed that the calibration curves remained practically unchanged with increasing settling time.

In order to verify the results obtained with photometer measurements, selected samples of 1 g SFH containing both dyed and undyed particles were spread in a thin layer on a sheet of white paper and photographed. Adobe Photoshop 2020 was used to analyze the photographs, determining the "average color" of each image. This procedure provided a further estimation of the proportion of dyed particles in each sample, and data was compared with results obtained using the photometer.

3. Results and Discussion

These are the results of the study on biomass particle mixing in an apparatus with vertical partitions during loop-like movement from feedstock loading to discharge.

Successive photographs of the particle bed from sample material collected at the outlet of the cold modeling apparatus at different time intervals following the introduction of dyed particles into the fluidized bed are presented in Figure 5.

The evolution of the concentration of dyed particles in samples collected at the outlet of the cold modeling apparatus at increasing retention times is presented in Figure 6. After 10 min, the sample collected at the outlet contained approximately 70% dyed particles. After 20 min, the outlet sample contained 100% dyed particles, indicating that all dyed particles had passed through the cold modeling apparatus. Accordingly, Figure 7 presents the evolution of the proportion of dyed particles in biomass samples, obtained by photographing samples using the methodology described above.

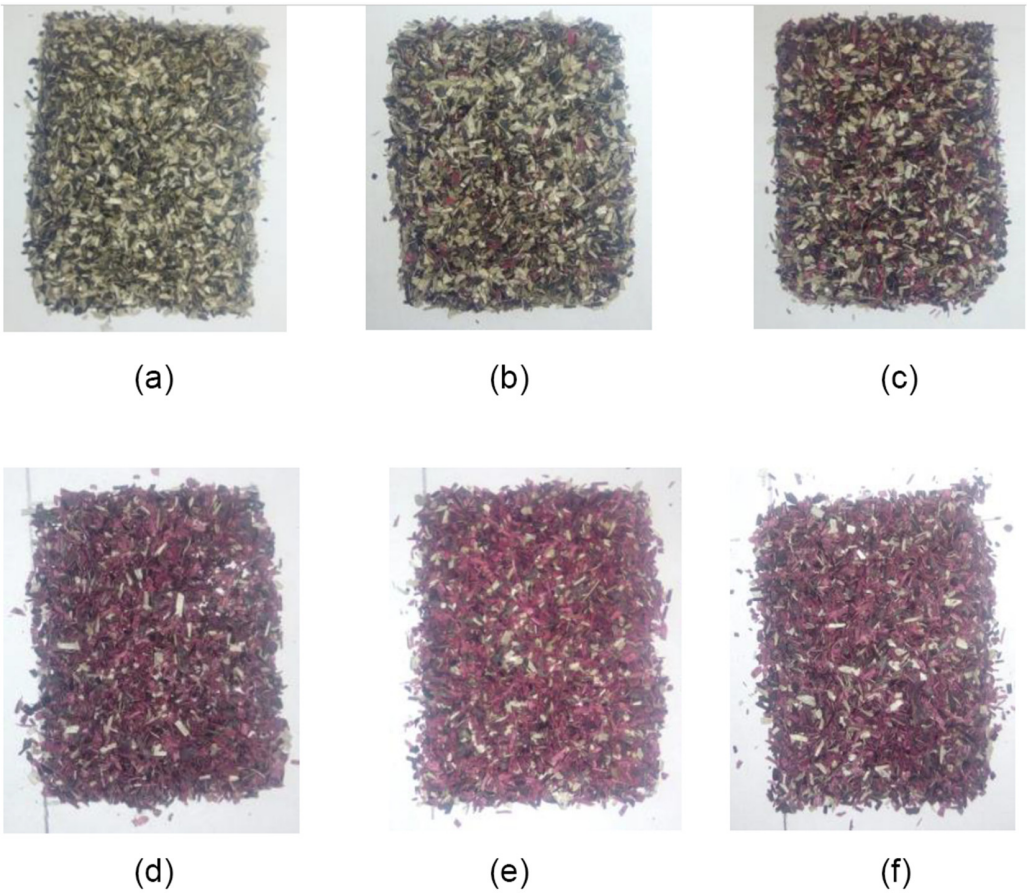

Figure 5. Successive photographs of the particle bed from samples collected at the outlet of the "cold" model at 30 (**a**), 150 (**b**), 300 (**c**), 600 (**d**), 900 (**e**), and 1200 s (**f**) after the introduction of dyed particles into the fluidized bed.

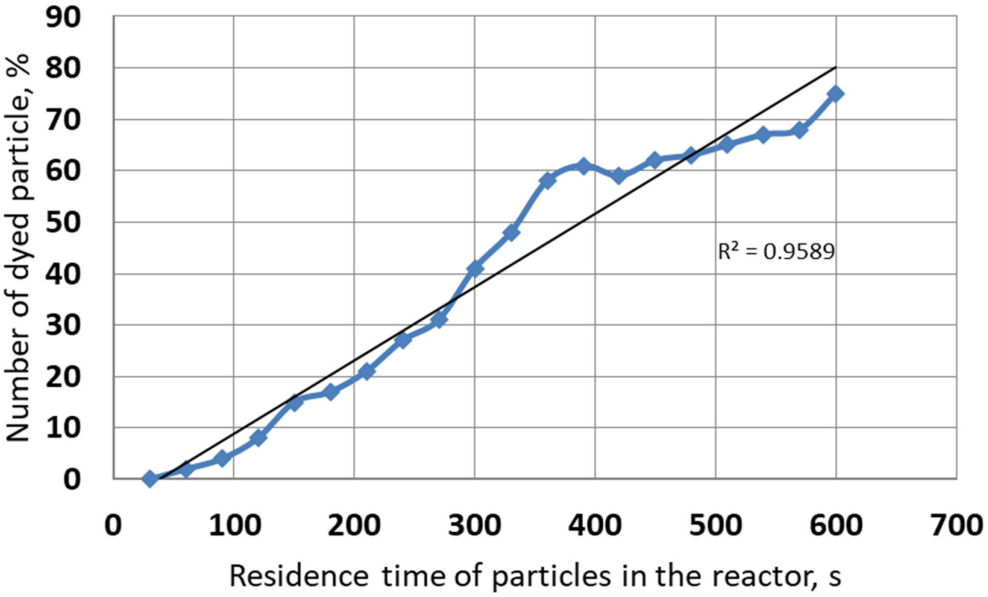

Figure 6. Evolution of the concentration of dyed particles in SFH samples collected at the outlet of the cold modeling apparatus, following their introduction at the inlet of the reactor.

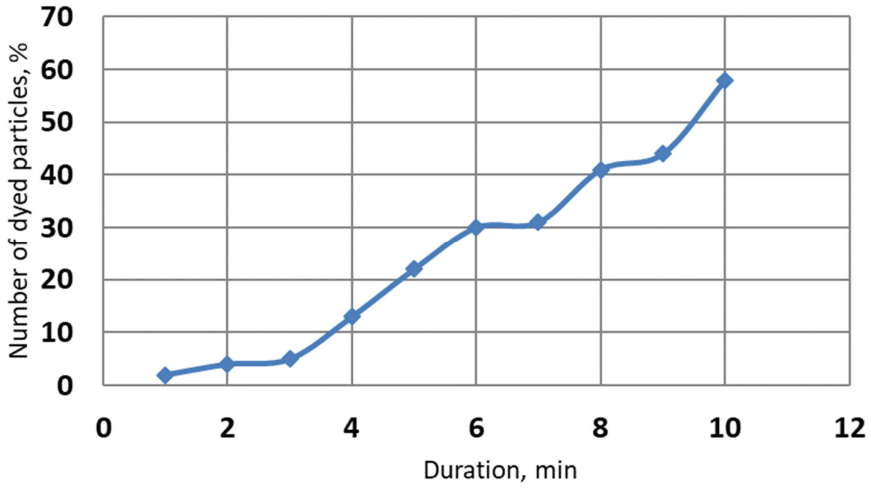

Figure 7. Proportion of dyed particles in SFH samples collected at the outlet of the cold modeling apparatus, following their introduction at the inlet of the reactor, according to photographs of the samples.

Comparison of the curves presented in Figures 6 and 7 indicates close agreement, confirming the experimental results obtained using the photometer.

Figure 8 presents the distribution of dyed particles in relation to residence time in the cold model apparatus.

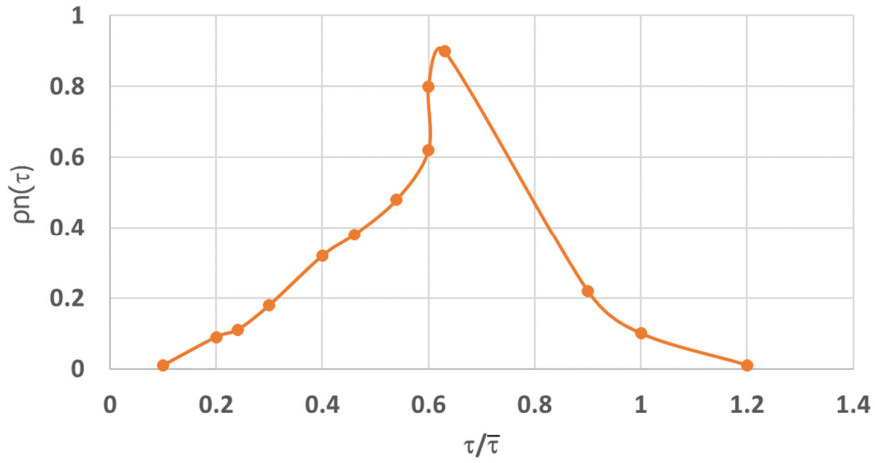

Figure 8. Density distribution curve of dyed particles in the "cold" reactor model.

The data presented in Figure 8 were processed using the method described by Levenspiel (1965) [26], according to the following stages:

1. The mean residence time of particles in the bed was determined.

$$\tau_0 = \frac{\sum \tau_i \cdot c_i}{\sum c_i}, \quad (4)$$

where τ_i—the time of measuring concentration c_i; c_i—the current concentration of dyed particles.

2. The dimensionless time and dimensionless concentration were calculated:

$$\tau_i^* = \frac{\tau_i}{\tau_0}; \; c_i^* = \frac{c_i}{c_0}; \quad (5)$$

where c_0—concentration of dyed particles at the outlet of the apparatus under steady-state conditions.

3. The expected value was determined:

$$\mu = \frac{\sum \tau_i^* \cdot c_i^*}{\sum c_i^*} - \mu^2 \quad (6)$$

and the distribution moment:

$$\sigma^2 = 2\frac{D}{\vartheta \cdot h} - 2\left(\frac{D}{\vartheta \cdot h}\right)^2 \cdot \left(1 - e^{-\frac{\vartheta \cdot h}{D}}\right). \quad (7)$$

4. Using Equation (7) and the method of successive approximations, the longitudinal particle mixing coefficient was determined: D = 7.23 × 10^{-4}.

The Peclet number was calculated using the formula:

$$Pe = \frac{\vartheta \cdot h}{D} = \frac{0.0238 \cdot 1.43}{7.23 \cdot 10^{-4}} = 47. \quad (8)$$

A relationship is known [26] that establishes a correlation between the Peclet criterion and the number of sections (N) in the pseudo-sectional model, in which a fluidized-bed apparatus is represented as a cascade of sequentially connected sections of equal volume, each operating under conditions of complete mixing.

$$N = \frac{Pe^2}{2 \times (Pe - 1 + \exp(-Pe))} = \frac{47^2}{2 \times (47 - 1 + \exp(-47))} = 24 \quad (9)$$

Thus, according to this methodology, to fully ensure operation of the reactor for torrefaction under ideal plug-flow conditions, the reactor would need to be equipped with 24 sections.

As presented in Figure 8, biomass particles are most likely to remain in a reactor with six vertical baffles for 6–8 min. Hence, it is logical to assume that in a reactor with 24 vertical baffles, biomass particles may remain in the reactor for 24–32 min.

Next, in batch reactor experiments, it was necessary to investigate the characteristics of biochar obtained at different durations of the thermal treatment process, including treatment for approximately 30 min.

Table 1 presents the results of studies on the physicochemical and thermal properties of the investigated biowastes after torrefaction in a superheated steam environment.

The residence time of biomass in the reactor has a significant effect on torrefaction outcomes in a superheated steam environment. The yield of torrefied biomass decreased with increasing residence time and reached minimum values of 44% for SFH. Increasing the residence time of both biomass types had a negligible effect on the yield of torrefied biomass yield at a temperature of 200 °C; however, at higher temperatures, it leads to a sharp reduction in yield. A similar behavior has been reported for conventional biomass torrefaction processes [27].

The higher heating value (HHV) of torrefied biomass was also influenced by the process temperature. At 300 °C, an increase in the processing time from 10 to 30 min resulted in a 1.38-fold increase in HHV.

Torrefaction temperature and processing duration may also affect other fuel characteristics of SFH.

In particular, for SFH, increasing the process temperature and residence time results in an increase in carbon content and a decrease in oxygen content.

The removal of volatile matter leads to an increase in fixed carbon content in torrefied biomass.

Table 1. Physicochemical and thermal characteristics of biowastes samples (as received) after torrefaction.

Name of Sample Characteristic	Torrefaction Parameters								
	200 °C			250 °C			300 °C		
	10 min	20 min	30 min	10 min	20 min	30 min	10 min	20 min	30 min
Biomass Type	**Sunflower Husk**								
Moisture, % (wt.)	3.86 ± 0.04	3.3 ± 0.03	2.9 ± 0.02	3.7 ± 0.02	3.2 ± 0.02	2.85 ± 0.01	3.3 ± 0.02	2.8 ± 0.01	2.5 ± 0.013
Ash content, % (wt.)	3.75 ± 0.07	3.9 ± 0.05	4.3 ± 0.03	5.38 ± 0.05	5.87 ± 0.06	6.8 ± 0.06	4.94 ± 0.05	6.3 ± 0.09	7.5 ± 0.07
Total sulfur, % (wt.)	0.02 ± 0.01	<0.01	<0.01	<0.01	<0.01	<0.01	<0.01	<0.01	<0.01
Total carbon, % (wt.)	52.1 ± 0.7	52.9 ± 0.3	54.5 ± 0.4	57.1 ± 0.3	58.7 ± 0.4	59.0 ± 0.5	57.7 ± 0.2	59.2 ± 0.3	59.8 ± 0.5
Total hydrogen, % (wt.)	5.56 ± 0.03	5.05 ± 0.05	4.94 ± 0.02	5.14 ± 0.09	5.0 ± 0.02	4.8 ± 0.11	5.29 ± 0.07	5.0 ± 0.03	4.75 ± 0.04
Nitrogen, % (wt.)	0.61 ± 0.02	0.56 ± 0.01	0.5 ± 0.03	0.52 ± 0.04	0.5 ± 0.03	0.48 ± 0.02	0.57 ± 0.02	0.5 ± 0.03	0.47 ± 0.01
Oxygen, % (wt.)	34.1 ± 0.12	34.28 ± 0.09	32.85 ± 0.11	28.15 ± 0.10	26.72 ± 0.17	26.06 ± 0.14	28.19 ± 0.14	26.19 ± 0.17	24.97 ± 0.15
Volatile Matter Content, VM, %	65.2 ± 0.17	63.6 ± 0.15	61.28 ± 0.16	63.3 ± 0.17	58.7 ± 0.14	54.42 ± 0.16	50.2 ± 0.14	44.9 ± 0.17	36.29 ± 0.12
Fixed Carbon Content, FC, %	27.19 ± 0.06	29.2 ± 0.09	31.52 ± 0.07	25.62 ± 0.07	32.23 ± 0.05	35.93 ± 0.09	41.56 ± 0.08	46.0 ± 0.06	53.71 ± 0.07
FR = FC/VM	0.42	0.46	0.51	0.4	0.55	0.66	0.83	1.02	1.48
H/C	1.28	1.24	1.18	1.08	1.02	0.98	1.1	1.01	0.95
O/C	0.49	0.49	0.45	0.37	0.34	0.33	0.37	0.33	0.31
Higher heating value on a dry, ash-free basis, HHV, MJ/kg	22.1	22.7	23.1	24.87	25.3	26.01	24.45	25.6	26.86
CI, MJ/kg	56.14	56.18	45.55	65.13	49.0	38.49	31.14	26.7	15.7
EF	1.13	1.16	1.18	1.27	1.3	1.33	1.25	1.31	1.38
MY, %	87	86	83	77	72	68	52	49	44
EY, %	97.18	99.76	97.94	97.79	93.6	90.44	65	64.19	88.58

In addition, the absolute fixed carbon concentration—defined as the product of biomass yield and fixed carbon content—also increased with increasing process temperature and processing duration. This indicates the conversion of a portion of volatile matter into fixed carbon during torrefaction [28].

A reduction in oxygen content in torrefied biomass was another advantage of the torrefaction process for SFH. The minimum oxygen content reached 24.97%. These values were comparable to the characteristics of torrefied biomass obtained using conventional torrefaction methods [29,30].

As shown in the Van Krevelen diagram (Figure 9), atomic H/C and O/C ratios decreased after torrefaction in superheated steam along the dehydration line. This suggests that dehydration may be the dominant reaction responsible for the removal of oxygenated compounds during superheated steam torrefaction of both SFH. Previous studies on superheated steam torrefaction of woody biomass have also reported significant decarbonization reactions contributing to oxygen removal [10,31].

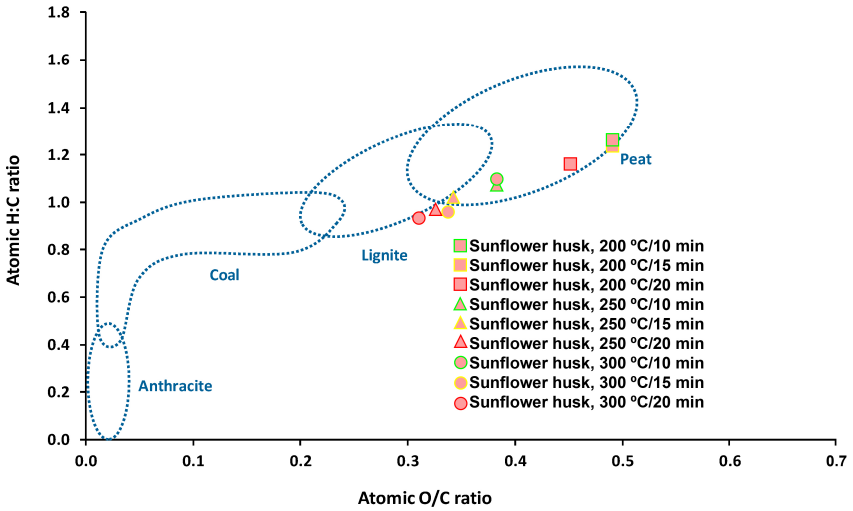

Figure 9. Van Krevelen diagram.

During torrefaction in superheated steam, holocellulose undergoes degradation accompanied by intensive water loss, resulting in dehydration being more pronounced than decarbonization. After torrefaction at 300 °C, the atomic H/C and O/C ratios of SFH decrease to the range characteristic of lignite and coal. Therefore, torrefied SFH can be considered a potential alternative solid fuel.

The fuel ratio (FR), calculated as $FR = FC/VM$ [31], increased with increasing processing time and torrefaction temperature, reaching its maximum value at 300 °C. The low FR values of the raw feedstock (0.42 for SFH) indicate that the untreated biomass is easy to ignite but difficult to control due to its high volatile matter content [31]. Superheated steam torrefaction enhances the fuel ratio, suggesting improved fuel properties, including a more stable flame and reduced smoke emission. Maximum FR values were achieved at a torrefaction temperature of 300 °C (1.48 for SFH). Fuel ratios below 2 FR < 2 are considered beneficial for ignition performance [32].

Combustion index [31] is another important parameter used to evaluate the combustion compatibility of solid fuels in blended systems.

$$\mathrm{CI\ (MJ/kg)} = \mathrm{HHV} \times (115 - \mathrm{Ash}) \times \mathrm{VM}/(105 \times \mathrm{FC}) \quad (10)$$

For raw material CI = 63.77 for SFH. It has been reported [33] that biofuels with CI values in the range of 12.56–22.03 MJ/kg are suitable for co-combustion with coal. According to this criterion, sunflower husk torrefied at 300 °C for 30 min may be suitable for co-combustion with coal.

Thus, torrefaction in a fluidized bed reactor under superheated steam conditions enables the production of high-quality biofuels from sunflower husk that are suitable, among other applications, for co-combustion with coal.

However, as will be shown below, the torrefaction conditions required to produce biofuels suitable for co-combustion with coal are not the most energy-efficient.

Table 1 also presents the values of mass yield (MY), energy densification factor (EF), and energy yield (EY).

The mass yield (MY) of torrefied biomass relative to raw biomass was calculated as follows, allowing for the evaluation of the mass loss resulting from torrefaction:

$$\mathrm{MY} = \mathrm{M_s}/\mathrm{M_r} \quad (11)$$

where M_r—weight of raw sample, M_s—weight of torrefied sample.

Furthermore, the enhancement factor (EF) of the higher heating value (HHV) of torrefied biomass (HHV s) compared with raw biomass (HHV r) was calculated as follows:

$$EF = (HHV\ s)/(HHV\ r) \quad (12)$$

Energy yield (EY) was calculated as follows, where maximal energy yield (EY) may correspond to optimal torrefaction conditions, for which the maximum increase in heating value can be achieved along with minimal weight loss of biomass [13]:

$$EY = MY \times EF \quad (13)$$

An example calculation for the EY is provided for the torrefaction of sunflower husk at a temperature of 300 °C for 10 min.

For this example, M_r = 800 g, M_s = 416 g, i.e., MY = M_s/M_r = 0.52.

HHV_r = 19.51 MJ/kg, HHV_s = 24.45 MJ/kg, i.e., EF = (HHV s)/(HHV r) = 1.25.

EY = MY × EF = 0.52 × 1.25 × 100% = 65%.

As shown in Table 1, the maximum torrefaction efficiency of sunflower husk—i.e., achieving the highest calorific value at maximum biochar yield—occurs in the temperature range of 200–250 °C. However, even within this range, the maximum torrefaction efficiency gradually decreases with increasing temperature and treatment duration. At a processing temperature of 300 °C, there is an extreme dependence of the torrefaction process efficiency on the processing duration: with an increase in the biomass processing duration to 20 min, the efficiency of the torrefaction process decreases due to an increase in the mass loss of the sample during processing; however, with an increase in the processing duration to 30 min, the efficiency of the torrefaction process again increases due to an increase in the combustion heat of the biomass.

These results are consistent with findings from other studies on the torrefaction of food waste [34]: during the torrefaction of pea husk, increasing the temperature from 250 to 450 °C led to a 1.32–2.26-fold increase in the calorific value compared to raw biomass, while the energy yield decreased from 97.75% at 250 °C to 82.73% at 450 °C. For peach pits, a similar temperature increase from 250 to 450 °C resulted in a 1.12–1.54-fold increase in HHV, whereas the EY declined from 99.76% at 250 °C to 59.05% at 450 °C.

It should also be noted that biomass torrefaction in a fluidized bed under a superheated steam atmosphere proceeds significantly faster than in reactors of other designs. For example, the torrefaction of biomass in a hearth-type reactor with a dense mechanically agitated bed has been repeatedly investigated by the authors [35]. Biochar with a carbon content of 54–59% can be produced in a hearth-type reactor within 60–120 min.

The analysis shows that the proposed reactor with 24 vertical baffles can be used to conduct the torrefaction process with maximum energy efficiency. However, strict control of the residence time of biomass particles in the reactor is necessary. This control should prevent both the bypass of insufficiently processed particles through the reactor and the retention of particles beyond the required processing time.

In a fluidized bed reactor, erosion and corrosion of the reactor walls, pipes immersed in the fluidized bed, etc. can be observed. Special coatings can be used to protect against such wear [36]. In this article we presented the results of full scale abrasion and corrosion resistance tests carried out on the experimental specimens of grade C 22 and S355J2 steels with protective Cr–CrC and Cr–CrN ion-plasma coatings (IPCs) after they have been held for 576 h in a 25 kW fluidized bed cyclone stoker operated on three kinds of pelletized biofuel: flax shives, straw, and sunflower husk. The temperature in the furnace and in the gas flue, in which the experimental specimens made of grade 09G2S and St20 steels were placed, rangd from 750 to 650 °C. A chemical analysis of the ash produced after

combusting these three kinds of pelletized fuel has shown that potassium and chlorine were available in the ash composition, the presence of which may give rise to the occurrence of corrosive compounds in the case of moisture condensation during the equipment outage periods. It has been found that the studied coatings did not experience abrasion or corrosion destruction; the coating thickness changed by a factor of 1.2–1.5 on average. A deviation in the morphology was noted as a consequence of coating surface layer oxidation at the maximal exposure time; however, no material oxidation under the coating was found on the transverse metallographic sections of the coated specimens. The bench tests of grade 09G2S steel specimens with protective Cr–CrN IPC carried out after holding them in the installation's furnace at an abrasive air flow incidence angle of 90° have shown that the abrasive resistance in terms of steady wear rate has increased by no less than a factor of two in comparison with that of non-coated specimens. In testing the corrosion resistance of specimens made of grade St20 steel with Cr–CrC coating after holding them in the installation's gas flue followed by holding them for 480 h in water extracted from the ash of each of the combusted biofuels, it has been noted that the corrosion rate determined using the gravimetric method has been decreased by 1.2–2.3 times in comparison with the same indicator of non-coated specimens. According to the study results, multilayer Cr–CrC and Cr–CrN ion-plasma coatings are promising for ensuring protection against corrosion and abrasion wear for the furnace and gas flue materials in fluidized bed boilers that use agricultural waste (flax shives, straw, or sunflower husk) as biofuel.

4. Conclusions

We proposed placing vertical partitions along the walls of a cylindrical reactor, which may allow for a significant reduction in reactor size for torrefaction, according to results obtained from a cold model. The transfer of biomass particles from one section of the reactor to another occurred along the full height of the partition through the gap between the partition and the reactor wall, minimizing the likelihood of agglomeration and particle accumulation in the lower part of the reactor.

The reactor of the proposed design can be used for the torrefaction of various types of biomasses, such as sunflower husks. Studies of the movement of dyed sunflower husk particles in a cold model of our reactor showed that, to operate the reactor in an ideal displacement mode ensuring complete processing of biomass particles, the reactor should be fitted with 24 vertical partitions.

Using sunflower husks (SFH) as example feedstock, we demonstrated that high-quality biofuel suitable for co-firing with coal may be obtained at a torrefaction temperature of 300 °C and a processing time of 30 min. This duration of torrefaction can be achieved in a reactor of our design operating in continuous mode. However, this conclusion must be confirmed by testing the reactor for the torrefaction of various types of biomasses.

Author Contributions: Conceptualization, F.T., A.R. and R.I.; methodology, O.M. and S.G.; validation, D.K. and A.M.; investigation, S.G. and D.K.; data curation, O.M.; writing—original draft preparation, F.T. and R.I.; writing—review and editing, R.I. and A.M.; visualization, E.P. and Y.T. All authors have read and agreed to the published version of the manuscript.

Funding: The study was carried out with the financial support of the Ministry of Science and Higher Education of Russia (Agreement No. 075-15-2024-628 dated 12 July 2024. Project name: "Development of technology to improve the efficiency and reliability of boilers burning biowaste in a fluidized bed of inert material". The head performer is the Federal State Budget Educational Institution of Higher Education National Research University "Moscow Power Engineering Institute").

Data Availability Statement: The data presented in this study are available on request from the corresponding author.

Conflicts of Interest: Author Fouzi Tabet was employed by the company Opti'Tech, Schletterstrasse. Authors Rafail Isemin and Alexander Mikhalev were employed by the company Clean Energy LLC. The remaining authors declare that the research was conducted in the absence of any. The remaining authors declare that the research was conducted in the absence of any.

Abbreviations

The following abbreviations are used in this manuscript:

SFH	Sunflower husk
FS	Flax shives
HHV	Higher heating value
MY	Mass yield
EF	Energy densification factor
EY	Energy yield

References

1. Soucek, J.; Jasinskas, A. Assessment of the Use of Potatoes as a Binder in Flax Heating Pellets. *Sustainability* **2020**, *12*, 10481. [CrossRef]
2. Perea-Moreno, M.-A.; Manzano-Agugliaro, F.; Perea-Moreno, A.-J. Sustainable Energy Based on Sunflower Seed Husk Boiler for Residential Buildings. *Sustainability* **2018**, *10*, 3407. [CrossRef]
3. Cubitto, M.A.; Gentili, A.R. Bioremediation of crude oil-contaminated soil by immobilized bacteria on an agroindustrial waste—Sunflower seed husks. *Bioremediat. J.* **2015**, *19*, 277–286. [CrossRef]
4. Brachi, P.; Miccio, F.; Miccio, M.; Ruoppolo, G. Torrefaction of tomato peel residues in a fluidized bed of inert particles and a fixed bed reactor. *Energy Fuels* **2016**, *30*, 4858–4868. [CrossRef]
5. Brachi, P.; Miccio, F.; Miccio, M.; Ruoppolo, G. Fluidized bed Torrefaction of Industrial Tomato Peels: Set-up of a New Batch Lab-Scale Test Rig and Preliminary Experimental Results. In Proceedings of the 22nd International Conference on Fluidized Bed Conversion, Turku, Finland, 14–17 June 2015; Volume 1, pp. 438–447.
6. Brachi, P.; Chirone, R.; Miccio, M.; Ruoppolo, G. Fluidized bed torrefaction of biomass pellets: A comparison between oxidative and inert atmosphere. *Powder Technol.* **2019**, *357*, 97–107. [CrossRef]
7. Wang, Z.; Li, H.; Lim, C.J.; Grace, J.R. Oxidative torrefaction of spruce-pine-fir sawdust in a slot-rectangular spouted bed reactor. *Energy Convers. Manag.* **2018**, *174*, 276–287. [CrossRef]
8. Funke, A.; Felix Reebs, F.; Kruse, A. Experimental comparison of hydrothermal and vapothermal carbonization. *Fuel Process. Technol.* **2013**, *115*, 261–269. [CrossRef]
9. Roy, B.; Kleine-Möllhoff, P.; Dalibard, A. Superheated Steam Torrefaction of Biomass Residues with Valorisation of Platform Chemicals—Part 1: Ecological Assessment. *Sustainability* **2022**, *14*, 1212. [CrossRef]
10. Zhang, D.; Chen, X.; Qi, Z.; Wang, H.; Yang, R.; Lin, W.; Li, J.; Zhou, W.; Ronsse, F. Superheated steam as carrier gas and the sole heat source to enhance biomass torrefaction. *Bioresour. Technol.* **2021**, *331*, 124955. [CrossRef]
11. Isemin, R.; Brulé, M.; Klimov, D.; Milovanov, O.; Mikhalev, A.; Silva, C.E.d.F.; Kuzmin, S.; Milovanov, K.; Guo, X. Conversion of Potato Peel into Solid Biofuel Through Torrefaction in a Fluidized Bed of Olivine Sand. *Energies* **2025**, *18*, 5496. [CrossRef]
12. Isemin, R.; Mikhalev, A.; Kuzmin, S.; Brulé, M.; Ainane, T.; Milovanov, O.; Klimov, D.; Milovanov, K. Comparison of Dry and Wet Torrefaction for Biochar Production from Olive Leaves and Olive Pomace. *Processes* **2025**, *13*, 2155. [CrossRef]
13. Wang, Z. Biomass Torrefaction in Slot–Rectangular Spouted Bed. Ph.D. Thesis, the University of British Columbia, Vancouver, BC, Canada, 2017.
14. Thengane, S.K.; Kung, K.S.; Gomez-Barea, A.; Ghoniem, A.F. Advances in biomass torrefaction: Parameters, models, reactors, applications, deployment, and market. *Prog. Energy Combust. Sci.* **2022**, *93*, 10104059. [CrossRef]
15. Grace, J.R. Introduction history applications. In *Essentials of Fluidization Technology*; Grace, J.R., Bi, X., Ellis, N., Eds.; Wiley: Hoboken, NJ, USA, 2020; pp. 1–9.
16. Xing, X.; Zhang, C.; Jiang, B.; Sun, Y.; Zhang, L.; Briens, C. Effect of a Baffle on Bubble Distribution in a Bubbling Fluidized Bed. *Processes* **2021**, *9*, 1150. [CrossRef]
17. Rennebaum, H.S.; Brummerloh, D.L.; Benders, S.; Penn, A. The effect of baffles on the hydrodynamics of a gas-solid fluidized bed studied using real-time magnetic resonance imaging. *Powder Technol.* **2024**, *432*, 119114. [CrossRef]
18. Phuakpunk, K.; Chalermsinsuwan, B.; Assabumrungrat, S. Reduction of bubble coalescence by louver baffles in fluidized bed gasifier. *Energy Rep.* **2022**, *8*, 96–106. [CrossRef]

19. Phuakpunk, K.; Chalermsinsuwan, B.; Assabumrungrat, S. Effect of louver baffles installation on hydrodynamics of bubbling fluidization in biomass gasifier. *Sci. Rep.* **2022**, *12*, 14891. [CrossRef]
20. Liu, N.; Liu, X.; Wang, F.; Xin, F.; Sun, M.; Zhai, Y.; Zhang, X. CFD simulation study of the effect of baffles on the fluidized bed for hydrogenation of silicon tetrachloride. *Chin. J. Chem. Eng.* **2022**, *45*, 219–228. [CrossRef]
21. Chen, K.; Bachmann, P.; Bück, A.; Jacob, M.; Tsotsas, E. CFD simulation of particle residence time distribution in industrial scale horizontal fluidized bed. *Powder Technol.* **2019**, *345*, 129–139. [CrossRef]
22. Bachmann, P.; Bück, A.; Tsotsas, E. Experimental investigation and correlation of the Bodenstein number in horizontal fluidized beds with internal baffles. *Powder Technol.* **2017**, *308*, 378–387. [CrossRef]
23. *ASTM E 870-82*; Standard Methods of Analysis of Wood Fuel. ASTM: West Conshohocken, PA, USA, 2019.
24. Milovanov, O.Y.; Isemin, R.L.; Mikhalev, A.V.; Klimov, D.V.; Kuzmin, S.N.; Muratova, N.S.; Sakovyh, A.E. Some Results of Preliminary Studies to Create an Industrial Reactor for Oxidative Torrefaction of Biowaste. *Chem. Eng. Trans.* **2020**, *80*, 55–59.
25. Ergun, S. Fluid flow through packed columns. *Chem. Eng. Prog.* **1952**, *48*, 89–94.
26. Levenspiel, O. *Chemical Reaction Engineering*; John Wiley and Sons, Inc.: New York, NY, USA; London, UK, 1965; pp. 269–277.
27. Sukiran, M.A.; Wan Daud, W.M.A.; Abnisa, F.; Nasrin, A.B.; Abdul Aziz, A.; Loh, S.K. A comprehensive study on torrefaction of empty fruit bunches: Characterization of solid, liquid and gas products. *Energy* **2021**, *230*, 120877. [CrossRef]
28. Zhang, D.; Han, P.; Zheng, H.; Yan, Z. Torrefaction of walnut oil processing wastes by superheated team: Effects on products characteristics. *Sci. Total Environ.* **2022**, *830*, 154649. [CrossRef] [PubMed]
29. Chiou, B.-S.; Valenzuela-Medina, D.; Bilbao-Sainz, C.; Klamczynski, A.K.; Avena-Bustillos, R.J.; Milczarek, R.R.; Du, W.X.; Glenn, G.M.; Orts, W.J. Torrefaction of pomaces and nut shells. *Bioresour. Technol.* **2015**, *177*, 58–65. [CrossRef]
30. Wang, C.; Yuan, X.; Li, S.; Zhu, X. Enrichment of phenolic products in walnut shell pyrolysis bio-oil by combining torrefaction pretreatment with fractional condensation. *Renew. Energy* **2021**, *169*, 1317–1329. [CrossRef]
31. Zhang, D.; Han, P.; Yang, R.; Wang, H.; Lin, W.; Zhou, W. Fuel properties and combustion behaviors of fast torrefied pinewood in a heavily loaded fixed-bed reactor by superheated steam. *Bioresour. Technol.* **2021**, *342*, 125929. [CrossRef]
32. Kongto, P.; Palamanit, A.; Chaiprapat, S.; Tippayawong, N. Enhancing the fuel properties of rubberwood biomass by moving bed torrefaction process for further applications. *Renew. Energy* **2021**, *170*, 703–713. [CrossRef]
33. Singh, R.K.; Sarkar, A.; Chakraborty, J.P. Effect of torrefaction on the physicochemical properties of pigeon pea stalk (Cajanus cajan) and estimation of kinetic parameters. *Renew. Energy* **2019**, *138*, 805–819. [CrossRef]
34. Isemin, R.; Tabet, F.; Shevchenko, A.; Mikhalev, A.; Kuzmin, S.; Mideksa, M.J.; Milovanov, O.; Klimov, D.; Milovanov, K.; Faleeva, Y.; et al. Assessment of the Influence of Temperature and Exothermic Effects During Torrefaction on the Properties of Agricultural Waste. *Processes* **2025**, *13*, 3294. [CrossRef]
35. Škorjanc, A.; Gruber, S.; Rola, K.; Goričanec, D.; Urbancl, D. Advancing Energy Recovery: Evaluating Torrefaction Temperature Effects on Food Waste Properties from Fruit and Vegetable Processing. *Processes* **2025**, *13*, 208. [CrossRef]
36. Ryzhenkov, A.V.; Mednikov, A.F.; Kachalin, G.V.; Tkhabisimov, A.B.; Zilova, O.S.; Grigor'ev, S.V.; Milovanov, K.I.; Buchilko, E.K. Results of Full-Scale Tests of Ion-Plasma Coatings in a Fluidized Bed Cyclone Stoker. *Therm. Eng.* **2025**, *72*, 968. [CrossRef]

Disclaimer/Publisher's Note: The statements, opinions and data contained in all publications are solely those of the individual author(s) and contributor(s) and not of MDPI and/or the editor(s). MDPI and/or the editor(s) disclaim responsibility for any injury to people or property resulting from any ideas, methods, instructions or products referred to in the content.